Scientific Research Publishing

Journal of Power and Energy Engineering, 2022, 10, 26-44
https://www.scirp.org/journal/jpee
ISSN Online: 2327-5901
ISSN Print: 2327-588X

# Reliability Analysis of Wind Energy Generation System Using Stochastic Method

**Godwin Diamenu[1], Joseph Cudjoe Attachie[1], Christian Kwaku Amuzuvi[2]**

[1]Electrical and Electronic Engineering Department, University of Mines and Technology (UMaT), Tarkwa, Ghana
[2]Renewable Energy Engineering Department, University of Mines and Technology (UMaT), Tarkwa, Ghana
Email: alcatelgodwin@yahoo.co.uk, jcattachie@umat.edu.gh, ckamuzuvi@umat.edu.gh

**How to cite this paper:** Diamenu, G., Attachie, J.C. and Amuzuvi, C.K. (2022) Reliability Analysis of Wind Energy Generation System Using Stochastic Method. *Journal of Power and Energy Engineering*, **10**, 26-44.
https://doi.org/10.4236/jpee.2022.108003

**Received:** May 23, 2022
**Accepted:** August 13, 2022
**Published:** August 16, 2022



## Abstract

Operators of renewable energy systems (RESs) must always manage uncertainty to some extent to ensure the reliability and the security of the electric power supply source. The guiding principle in this regard is to ensure service reliability and quality by balancing load variations with the variable renewable energy (VRE) sources. If the power generated by these VRE sources is not properly managed in conjunction with the varying load, the power grid may fail to achieve the required balance. To ensure its reliable operation, reliability analysis is vital for wind energy generation system (WEGS). This paper evaluated and assessed the reliability of WEGS and a proposed varying load by first using a stochastic approach to model the WEGS and the proposed varying load after which power generation indices were used to evaluate and assess the performance of the model. The WEGS and the varying load were modelled separately after which the two were combined into one model. Full availability, partial availability, the expected energy not supplied (EENS) or loss of energy expectation (LOEE), the mean or average instantaneous electric power generation and mean instantaneous generation deficiency were the indices used for the evaluation of the WEGS. The results indicated that the electric power generation will meet the power demand during most of the transition states of the WEGS with the expectation that the variation in the load will not be at fast pace and in large quantum.

## Keywords

Renewable Energy, Stochastic, Reliability, Availability, Transition Rate, Transition State

## 1. Introduction

Power generation from low carbon energy resources has significantly increased

in recent times. Wind energy is an important component of future energy systems to meet growing energy demands. The demand for wind energy is growing rapidly all over the world. According to the Global Wind Energy Council (GWEC), by the year 2020, 350 GW of wind power capacity would have been installed. According to European Wind Energy Association (EWEA), an increment of about 320 GW is expected in European wind power capacity by the year 2030 [1]. With the push to adopt more renewable energy resources (RERs), the total installed capacity of wind power throughout the world has exceeded 742.689 GW to date [2].

Fossil fuels are non-renewable and their associated prices keep fluctuating on the World. The increasing environmental and climatic conditions associated with fossil fuel usage had moved the research focus from conventional electricity resources to RERs. RERs, such as wind, solar energy from the sun, tidal wave, biomass from plants, small hydro sources and geothermal power, are clean alternatives to fossil fuels. Among them, wind energy is one of the most promising and rapidly developing RERs in the world today. The main attractions of wind energy are its naturally free availability everywhere and its low environmental impact [3]. Wind velocity determines the output of wind turbine generators (WTGs). Wind farms' production output is stochastic and completely different from that of conventional power generating units due to the fast changing and unpredictable characteristics of wind velocity and the random nature of WTG failures. Wind power generation's large variations are mostly caused by real-time changes in meteorological conditions [4].

Large-scale deployment of variable renewable energy (VRE) is associated with reliability and availability concerns. Wind energy generation system (WEGS) reliability and availability are vital and necessary requirements for meeting electric power demand [5]. Reliability is the ability of a system to perform its required function without failure, for a given time interval under given conditions, whereas availability is the ability to be in a state to perform as required [6]. To ensure its reliable operation, reliability analysis is vital for WEGS. In the last two decades, reliability evaluation methods for electric power systems, including VRE sources, have been developed.

The Markov model gives a simple description of a component, which is normally handled with mathematical methods. In order to be able to utilise it, the components of the system must be able to be described as a Markov model. This means that the system should be represented as a system lacking memory of previous states with identifiable system states. The system's reliability can then be evaluated using techniques based on the principles of the $K$ state Markov process. For this purpose, the state probabilities can only be obtained by solving $K$ differential equations either analytically or numerically [4].

The reliability analysis techniques based on the Markov chain process may be classified into two time domain modes: discrete and continuous, and reliability analysis in these two modes can be performed using the system state transition diagram. The Markov process had been utilised to derive the probability value of

each working state, the failure state, and the time required for the system to reach a steady state in reliability assessment over the years [7] [8].

A lot of reliability analysis of wind turbine (WT) system has been performed using WT components failure rates and restoration rates data in the literature. However, in the literature, there is no large-scale model for the study and evaluation of WEGS and a varying load. In this study, by means of different states and transitions between them, this paper is an insight into the performance analysis of WEGS and its accompanying varying load presented through a Markov model. The WEGS and the varying load were modelled separately. The two models were then combined into one model which was used to evaluate the generation indices. WEGS availability, expected energy not supplied (EENS) among others was performed using WT transition states due to the varying wind velocity.

## 2. The Proposed Modelling Approach

The Markov process approach is widely used to model the states of continuous and discrete stochastic processes of complex systems based on which the system reliability is ascertained. Markov process is a stochastic process evolving under the Markov property. The future state of the Markov process depends on the current state, it is conditionally independent of the past states of the stochastic process. Given a state $X_k$, the state $X_{k+i}$, where $i > 0$ are independent of state $X_{k-j}$ where $j > 0$ [4] [8]. The Markov model is a method based on states and the transitions between them. There are two main assumptions that are associated with Markov model:

- The system which is modelled by Markov process approach is memory-less. Thus, the future probability of each event is a function of the current state and it is independent from the former transitions to reach the new state.
- The probability of transition between states is assumed to be constant.

A three state Markov chain system transition diagram is given in **Figure 1**. State '0' represents the normal working state, and states "1" and "2" respectively represents partial and abnormal working states under different subsystem failure conditions.

For the three-state repairable system in **Figure 1**, the system state function is given as follows:

$$W(t)=\begin{cases}0, \text{ normal working state}\\ 1, \text{ partial working state}\\ 2, \text{ faulty working state}\end{cases}$$

where, $\lambda$ is failure rate of the system, $\mu$ is the repair rate of the system, $\Delta t$ is the represents a very short time interval.

Based on the state transition diagram given in **Figure 1**, the state transition matrix equation in the time interval $[t, t+\Delta t]$ for the system for each state represented by an $r$-by-$r$ transition matrix based on the transitions between the states is derived as follows:

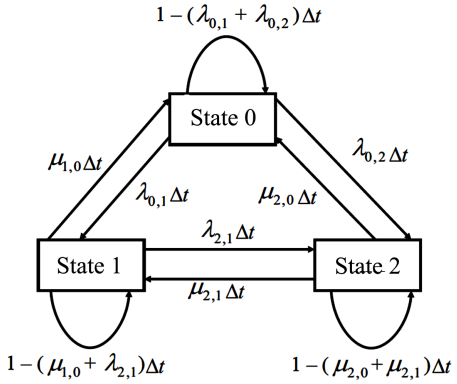


**Figure 1.** Three state system transition diagram.

$$\begin{bmatrix} P_0(t+\Delta t) \\ P_1(t+\Delta t) \\ P_2(t+\Delta t) \end{bmatrix} = \begin{bmatrix} 1-(\lambda_{0,1}+\lambda_{0,2}) & \mu_{1,0} & \mu_{2,0} \\ \lambda_{0,1} & 1-(\mu_{1,0}+\lambda_{2,1}) & \mu_{2,1} \\ \lambda_{0,2} & \lambda_{2,1} & 1-(\mu_{2,0}+\mu_{2,1}) \end{bmatrix} \begin{bmatrix} P_0(t) \\ P_1(t) \\ P_2(t) \end{bmatrix} \quad (1)$$

By taking the limit as $\Delta t \to 0$ in Equation (1), the differential equations of the system state probabilities are obtained as follows:

$$\begin{cases} \dfrac{\mathrm{d}p_0}{\mathrm{d}t} = \text{limit}_{\Delta\to 0} \dfrac{p_0(t+\Delta t)}{\Delta t} = 1-(\lambda_{0,1}+\lambda_{0,2})p_0(t)+\mu_{1,0}p_1(t)+\mu_{2,0}p_2(t) \\ \dfrac{\mathrm{d}p_1}{\mathrm{d}t} = \text{limit}_{\Delta\to 0} \dfrac{p_1(t+\Delta t)}{\Delta t} = \lambda_{0,1}p_0(t)+1-(\mu_{1,0}+\lambda_{2,1})p_1(t)+\mu_{2,1}p_2(t) \\ \dfrac{\mathrm{d}p_2}{\mathrm{d}t} = \text{limit}_{\Delta\to 0} \dfrac{p_2(t+\Delta t)}{\Delta t} = \lambda_{0,2}p_0(t)+\lambda_{2,1}p_1(t)+1-(\mu_{2,0}+\mu_{2,1})p_2(t) \end{cases} \quad (2)$$

where, the subscripts indicate the state the transition emanates from, and the next state it is going to terminate. Where, $P_0$ is the probability of the system being in normal working state, $P_1$ and $P_2$ is the system being in partial and abnormal working states respectively.

For the four-state repairable system in **Figure 2**, its state function is given as follows.

$$W(t) = \begin{cases} 0, \text{ normal working state (fully available)} \\ 1, \text{ partial working state (partially available)} \\ 2, \text{ degraded state (some how available to an extent)} \\ 3, \text{ faulty state (not available)} \end{cases}$$

**Figure 2** is a four state transition diagram for a Markov chain process. The state transition matrix equation in the time interval $[t, t+\Delta t]$ for the system for each state represented by an $r$-by-$r$ transition matrix based on the transitions between the states is derived as follows:

$$\begin{bmatrix} P_0(t+\Delta t) \\ P_1(t+\Delta t) \\ P_2(t+\Delta t) \\ P_3(t+\Delta t) \end{bmatrix} = \begin{bmatrix} 1-(\lambda_{0,1}+\lambda_{0,2}) & \mu_{1,0} & \mu_{2,0} & 0 \\ \lambda_{0,1} & 1-(\mu_{1,0}+\lambda_{1,3}) & 0 & \mu_{3,1} \\ \lambda_{0,2} & 0 & 1-\mu_{2,0} & 0 \\ 0 & \lambda_{1,3} & 0 & 1-\mu_{3,1} \end{bmatrix} \begin{bmatrix} P_0(t) \\ P_1(t) \\ P_2(t) \\ P_3(t) \end{bmatrix} \quad (3)$$

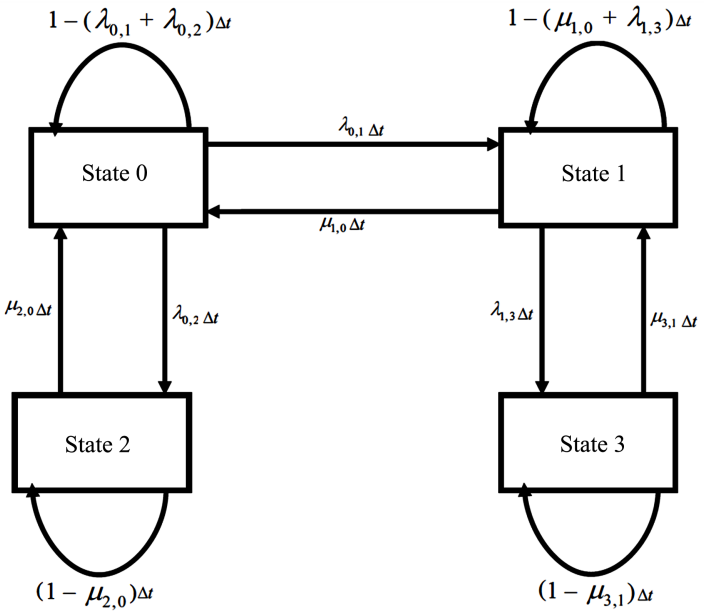


**Figure 2.** A four-state system transition diagram.

where, the subscripts indicate the state the transition emanates from, and the next state it is going to terminate, $\lambda$ is the failure rate of the system, $\mu$ is the repair rate of the system, $\Delta t$ is very short time interval, $P_0$ is the probability of the system being in normal working state, $P_1$ is the probability of the system being in partial working state, $P_2$ is the probability of the system being in degraded state, $P_3$ is the probability of the system being in abnormal working state.

By taking the limit as $\Delta t \to 0$ in Equation (3), the differential equations of the system state probabilities is obtained as follows:

$$\begin{cases} \dfrac{\mathrm{d}p_0}{\mathrm{d}t} = \operatorname{limit}_{\Delta t\to 0}\dfrac{p_0(t+\Delta t)}{\Delta t} = 1-\left(\lambda_{0,1}+\lambda_{0,2}\right)p_0(t)+\mu_{1,0}p_1(t)+\mu_{2,0}p_2(t)+0p_3(t) \\ \dfrac{\mathrm{d}p_1}{\mathrm{d}t} = \operatorname{limit}_{\Delta t\to 0}\dfrac{p_1(t+\Delta t)}{\Delta t} = \lambda_{0,1}p_0(t)+1-\left(\mu_{1,0}+\lambda_{1,3}\right)p_1(t)+0p_2(t)+\mu_{3,1}p_3(t) \\ \dfrac{\mathrm{d}p_2}{\mathrm{d}t} = \operatorname{limit}_{\Delta t\to 0}\dfrac{p_2(t+\Delta t)}{\Delta t} = \lambda_{0,2}p_0(t)+0p_1(t)+1-\mu_{2,0}p_2(t)+0p_3(t) \\ \dfrac{\mathrm{d}p_3}{\mathrm{d}t} = \operatorname{limit}_{\Delta t\to 0}\dfrac{p_3(t+\Delta t)}{\Delta t} = 0p_0(t)+\lambda_{1,3}p_1(t)+0p_2(t)+1-\mu_{3,1}p_3(t) \end{cases} \tag{4}$$

## 3. Case Study

To validate the proposed model, a four-state WEGS model with a four-state load model is proposed. The proposed modelling framework and the reliability analysis procedure is given by **Figure 3**.

### 3.1. WEGS Model

The model for the WEGS is made up of wind farms comprising a number of WTs. It is a four-state and eight-transition states model where a certain amount

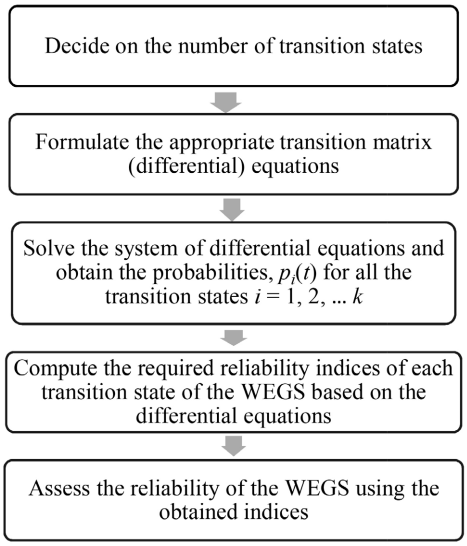


**Figure 3.** Framework procedure for the of reliability analysis of a typical WEGS.

of electric power is generated at each state to feed the electric load. The states are based on the WT power output curve given in **Figure 4**, which establishes a relation between the wind speed at its hub height and the power that can be extracted from the wind and injected into the power grid. It is very useful for evaluating the WT performance [9]. Even though it has cut-in, rated and cut-out speeds, another speed range is introduced between the cut-in speed and the rated speed which is known as the mid-range speed resulting in the four-state transition states instead of the original three-state transition states. The transition state diagram based on the WT output power curve is given in **Figure 5**. **Table 1** gives the wind speed and the assumed electric power generated during each state. The analysis assumed that no electric power is produced when the wind speed is below the cut-in speed.

The assumed transition rates among the various states of the WEGS is given by the transition rate matrix, $M$ defined as:

$$M = \left(m_{ij}\right) = \begin{pmatrix} 0.247 & 0.284 & 0.302 & 0.167 \\ 0.276 & 0.249 & 0.235 & 0.240 \\ 0.348 & 0.324 & 0.233 & 0.095 \\ 0.175 & 0.121 & 0.302 & 0.402 \end{pmatrix} \tag{5}$$

The assumed transition rate matrix is chosen in such a way that every row sum up to one which is in line with how the transition of the electric power demand occurs in the electric power and electric power demand combined model given by **Figure 7**, where an arrow indicates the direction of the electric power generation transition states (row wise) and electric power demand transition states (column wise) respectively.

## 3.2. Model for the Electric Power Demand

In reliability analysis, the model for the proposed load is very necessary since it indicates the electric power demand that must be met by the generation source.

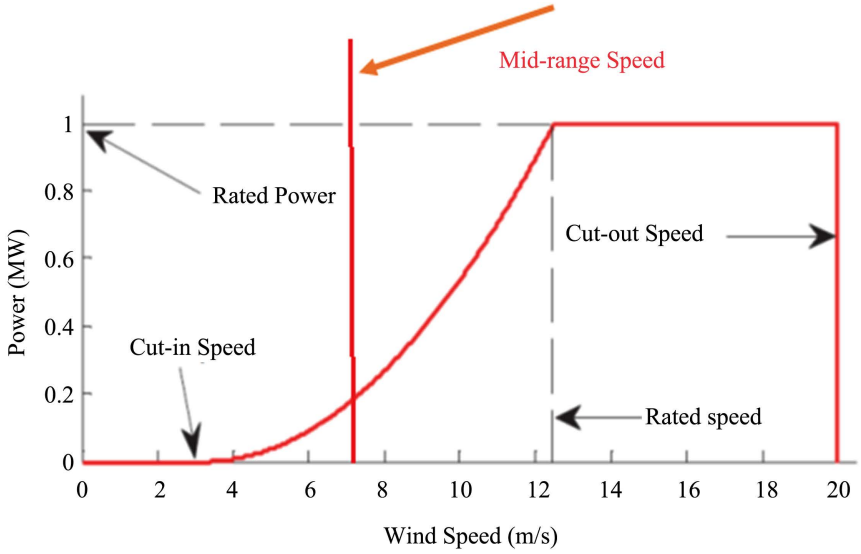


**Figure 4.** Wind turbine output power curve.

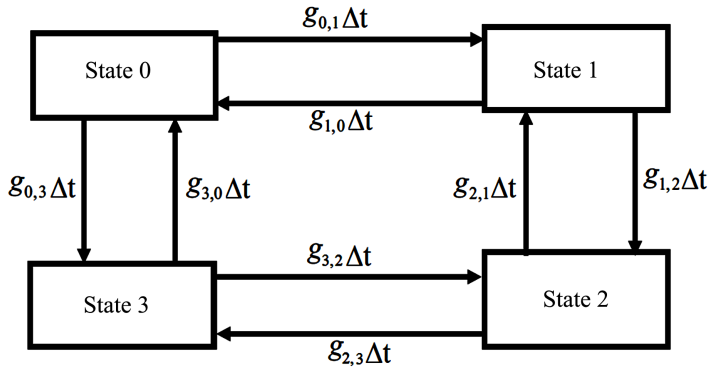


**Figure 5.** A four-state transition diagram for WEGS.

**Table 1.** Electric power produced by the WEGS during each state.

| S/No. | Wind Speed | Transition States | Electric Power Generated (MW) |
|---|---|---|---|
| 1 | 3.50 - 6.50 m/s | State 0 | 10 |
| 2 | 6.50 - 8.50 m/s | State 1 | 120 |
| 3 | 8.5 - 14.5 m/s | State 2 | 200 |
| 4 | 14.5 - 18.5 m/s | State 3 | 40 |

The transition can occur between two states at any particular time. An electric power system must match generation and load in real time. The electric power demand that must be met by the generation source fluctuates within certain time interval. Hence, in modelling the electric power demand or the load, uncertainty or randomness must be taken into consideration. The state transition diagram for the varying electric load is given in **Figure 6** indicating four different states comprising different load capacities as given in **Table 2**. The electric power load is assumed to be varying between the stated minimum and maximum values.

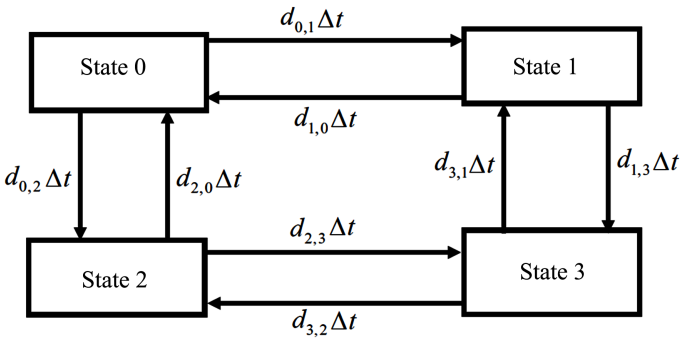


**Figure 6.** A four-state transition diagram for a varying electric power demand.

**Table 2.** Varying power demand states for reliability analysis.

| S/No. | Transition States | Electric Power Demand (MW) |
|---|---|---|
| 1 | State 0 | 50 |
| 2 | State 1 | 100 |
| 3 | State 2 | 140 |
| 4 | State 3 | 160 |

The assumed transition rates among the various states of the electric power demand is given by the transition rate matrix, $N$ defined as:

$$N = \left(n_{ij}\right) = \begin{pmatrix} 0.18 & 0.19 & 0.32 & 0.23 \\ 0.24 & 0.31 & 0.29 & 0.30 \\ 0.25 & 0.28 & 0.21 & 0.27 \\ 0.33 & 0.22 & 0.18 & 0.20 \end{pmatrix} \tag{6}$$

The assumed transition rate matrix is chosen in such a way that every column sum up to one which is in line with how the transition of the electric power demand occurs in the combined electric power generation and electric power demand model given by **Figure 7**.

### 3.3. Combined WEGS and Electric Power Demand Model

The objective of WEGS is to deliver the generation capacity to the load, it is possible to combine the equivalent transition diagram of the generation subsystem with the equivalent transition diagram of the electric power load subsystem. The states transition diagram for the WEGS and an electric power demand combined is given in **Figure 7**.

For a combined WEGS and the electric power demand, the output of the WEGS is represented by $a$ number of an electric power generation states and corresponding transition rate matrix is given by $M = [m_{ij}]$. That of the electric power demand is represented by $b$ number of transition states with the corresponding transition rate matrix given by $N = [n_{ij}]$. With the number of transition states for the WEGS being $a$, and that of the electric power demand being $b$, the total number of transition states for the WEGS and that of the electric power load combined is $a \times b$ transition states [10] [11]. The transition states for the

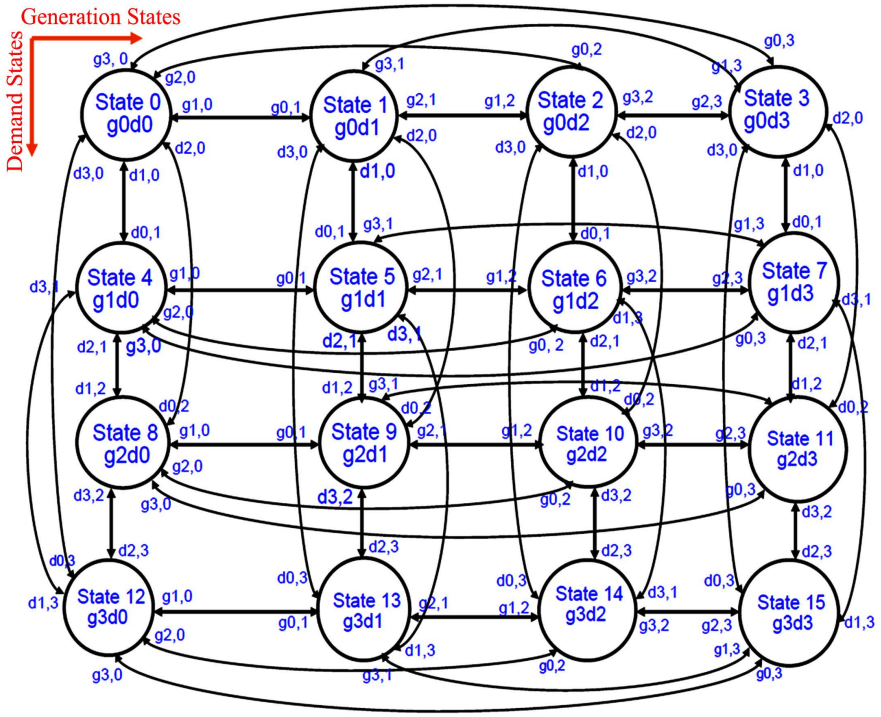


**Figure 7.** State-transition diagram for the combined WEGS and the electric power demand.

WEGS is given by $g \in (g_0, g_1, g_2, g_3)$ and that of the electric power demand is also given by $d \in (d_0, d_1, d_2, d_3)$. For this case study, the number of transition states of the WEGS and that of the electric power demand together gives sixteen (16) transition states. The state transition diagram for the combined WEGS and the electric power demand model is given in **Figure 7**. The horizontal transition states represent the power generation states of the wind farms in increasing order from left to right columns and the vertical transition states represents the demand states of the load. It is a state-transition-rate diagram as opposed to a state-transition diagram because it shows the rate at which the process moves from state to state and not the probability of moving from one state to another [12]. More than one transition cannot occur at a time. The combined electric power generation and electric power demand model has 16 transition states, which are categorized into two different classes, states (1, 2, 5, 6, 9, 10, 13, 14) that fully meets the electric power demand irrespective of the state in which it is, and those states (0, 3, 4, 7, 8, 11, 12. 15) that partially meets the electric power demand. The power generation and power demand at the various transition states is given in **Table 3**.

A graph of electric power generation and power demand at the various transition states against the various probabilities at those transition states is given by **Figure 8**.

The probabilities, $p_i(t)$, $0 \le i \le 15$ of the combined WEGS and electric power demand of the WEGS at the various states at the time, $t + \Delta$ are:

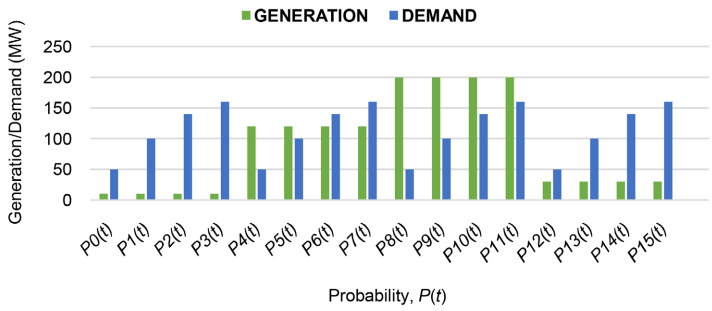


**Figure 8.** Electric power generation, power demand against probability plot.

**Table 3.** Power generation and power demand at the various transition states.

| States | Probabilities, $P(t)$ | Electric Power Generation (MW) | Electric Power Demand (MW) |
|---|---|---|---|
| 0 | $p_0(t)$ | 10 | 50 |
| 1 | $p_1(t)$ | 10 | 100 |
| 2 | $p_2(t)$ | 10 | 140 |
| 3 | $p_3(t)$ | 10 | 160 |
| 4 | $p_4(t)$ | 120 | 50 |
| 5 | $p_5(t)$ | 120 | 100 |
| 6 | $p_6(t)$ | 120 | 140 |
| 7 | $p_7(t)$ | 120 | 160 |
| 8 | $p_8(t)$ | 200 | 50 |
| 9 | $p_9(t)$ | 200 | 100 |
| 10 | $p_{10}(t)$ | 200 | 140 |
| 11 | $p_{11}(t)$ | 200 | 160 |
| 12 | $p_{12}(t)$ | 40 | 50 |
| 13 | $p_{13}(t)$ | 40 | 100 |
| 14 | $p_{14}(t)$ | 40 | 140 |
| 15 | $p_{15}(t)$ | 40 | 160 |

$$\left[P_0(t+\Delta t)\right]=\left[\left(1-g_{01}+g_{02}+g_{03}+d_{01}+d_{02}+d_{03}\right)\Delta tP_0(t)+g_{10}\Delta tP_1(t)+g_{20}\Delta tP_2(t)+g_{30}\Delta tP_3(t)+d_{10}\Delta tP_4(t)+d_{20}\Delta tP_8(t)+d_{30}\Delta tP_{12}(t)\right]\left[P_0(t)\right] \tag{7}$$

$$\left[P_1(t+\Delta t)\right]=\left[g_{01}\Delta tP_0(t)+\left(1-g_{10}+g_{12}+g_{13}+d_{01}+d_{02}+d_{03}\right)\Delta tP_1(t)+g_{21}\Delta P_2(t)+g_{31}\Delta tP_3(t)+d_{10}\Delta tP_5(t)+d_{20}\Delta tP_9(t)+d_{30}\Delta tP_{13}(t)\right]\left[P_1(t)\right] \tag{8}$$

$$\left[P_2(t+\Delta t)\right]=\left[g_{12}\Delta tP_0(t)+g_{02}P_1(t)\Delta t+(1-g_{20}+g_{21}+g_{23}+d_{01}+d_{02}+d_{03})\Delta tP_2(t)+g_{32}\Delta tP_3(t)+d_{10}\Delta tP_6(t)+d_{20}\Delta tP_{10}(t)+d_{30}\Delta tP_{14}(t)\right]\left[P_2(t)\right] \quad (9)$$

$$\left[P_3(t+\Delta t)\right]=\left[g_{03}\Delta tP_0(t)+g_{13}\Delta tP_1(t)+g_{13}\Delta tP_2(t)(1-g_{30}+g_{31}+g_{32}+d_{01}+d_{02}+d_{03})\Delta tP_3(t)+P_7(t)d_{10}\Delta t+P_{11}(t)d_{02}\Delta t+P_{15}(t)d_{30}\Delta t\right]\left[P_3(t)\right] \quad (10)$$

$$\left[P_4(t+\Delta t)\right]=\left[(1-g_{01}+g_{02}+g_{03}+d_{10}+d_{12}+d_{13})\Delta tP_4(t)+g_{10}\Delta tP_5(t)+g_{20}\Delta tP_6(t)+g_{30}\Delta tP_7(t)+d_{01}\Delta tP_0(t)+d_{21}\Delta tP_8(t)+d_{31}\Delta tP_{12}(t)\right]\left[P_4(t)\right] \quad (11)$$

$$\left[P_5(t+\Delta t)\right]=\left[(1-g_{10}+g_{12}+g_{13}+d_{10}+d_{12}+d_{13})\Delta tP_5(t)+g_{01}\Delta tP_4(t)+g_{21}\Delta tP_6(t)+g_{31}\Delta tP_7(t)+d_{01}\Delta tP_1(t)+d_{21}\Delta tP_9(t)+d_{31}\Delta tP_{13}(t)\right]\left[P_5(t)\right] \quad (12)$$

$$\left[P_6(t+\Delta t)\right]=\left[(1-g_{20}+g_{21}+g_{23}+d_{10}+d_{12}+d_{13})\Delta tP_6(t)+g_{02}\Delta tP_4(t)+g_{12}\Delta tP_5(t)+g_{32}\Delta tP_7(t)+d_{01}\Delta tP_2(t)+d_{21}\Delta tP_{10}(t)+d_{31}\Delta tP_{14}(t)\right]\left[P_6(t)\right] \quad (13)$$

$$\left[P_7(t+\Delta t)\right]=\left[(1-g_{30}+g_{31}+g_{32}+d_{10}+d_{12}+d_{13})\Delta tP_7(t)+g_{03}\Delta tP_4(t)+g_{13}\Delta tP_5(t)+g_{23}\Delta tP_6(t)+d_{01}\Delta tP_3(t)+d_{21}\Delta tP_{11}(t)+d_{31}\Delta tP_{13}(t)\right]\left[P_7(t)\right] \quad (14)$$

$$\left[P_8(t+\Delta t)\right]=\left[(1-g_{01}+g_{02}+g_{03}+d_{20}+d_{21}+d_{23})\Delta tP_8(t)+g_{10}\Delta tP_9(t)+g_{20}\Delta tP_{10}(t)+g_{30}\Delta tP_{11}(t)+d_{02}\Delta tP_0(t)+d_{12}\Delta tP_4(t)+d_{32}\Delta tP_{12}(t)\right]\left[P_8(t)\right] \quad (15)$$

$$\left[P_9(t+\Delta t)\right]=\left[g_{01}\Delta tP_8(t)+(1-g_{10}+g_{12}+g_{13}+d_{20}+d_{23}+d_{21})\Delta tP_9(t)+g_{21}\Delta tP_{10}(t)+g_{31}\Delta tP_{11}(t)+d_{02}\Delta tP_1(t)+d_{12}\Delta tP_5(t)+d_{32}\Delta tP_{13}(t)\right]\left[P_9(t)\right] \quad (16)$$

$$\left[P_{10}(t+\Delta t)\right]=\left[g_{02}\Delta tP_8(t)+g_{12}\Delta tP_9(t)+(1-g_{20}+g_{21}+g_{23}+d_{20}+d_{21}+d_{23})\Delta tP_{10}(t)+g_{32}\Delta tP_{11}(t)+d_{02}\Delta tP_2(t)+d_{12}\Delta tP_6(t)+d_{32}\Delta tP_{14}(t)\right]\left[P_{10}(t)\right] \quad (17)$$

$$\left[P_{11}(t+\Delta t)\right]=\left[g_{03}\Delta tP_8(t)+g_{13}\Delta tP_9(t)+g_{23}\Delta tP_{10}(t)+(1-g_{30}+g_{31}+g_{32}+d_{10}+d_{21}+d_{23})\Delta tP_{11}(t)+d_{01}\Delta tP_3(t)+d_{12}\Delta tP_7(t)+d_{32}\Delta tP_{15}(t)\right]\left[P_{11}(t)\right] \quad (18)$$

$$\left[P_{12}(t+\Delta t)\right]=\left[(1-g_{01}+g_{02}+g_{03}+d_{30}+d_{31}+d_{32})\Delta tP_{12}(t)+P_{13}(t)g_{10}\Delta t+P_{14}(t)g_{20}\Delta t+g_{30}\Delta tP_{15}(t)+d_{03}\Delta tP_0(t)+d_{13}\Delta tP_4(t)+d_{23}\Delta tP_8(t)\right]\left[P_{12}(t)\right] \quad (19)$$

$$\left[P_{13}(t+\Delta t)\right]=\left[g_{01}\Delta tP_{12}(t)+(1-g_{10}+g_{12}+g_{13}+d_{30}+d_{31}+d_{32})\Delta tP_{13}(t)+g_{21}\Delta tP_{14}(t)+g_{31}\Delta tP_{15}(t)+d_{03}\Delta tP_1(t)+d_{13}\Delta tP_5(t)+d_{23}\Delta tP_9(t)\right]\left[P_{13}(t)\right] \quad (20)$$

$$\left[P_{14}(t+\Delta t)\right]=\left[g_{02}\Delta tP_{12}(t)+g_{12}\Delta tP_{13}(t)+(1-g_{20}+g_{21}+g_{23}+d_{30}+d_{31}+d_{32})\Delta tP_{14}(t)+P_{15}(t)g_{32}\Delta t+d_{03}\Delta tP_2(t)+d_{13}\Delta tP_6(t)+d_{23}\Delta tP_{10}(t)\right]\left[P_{14}(t)\right] \quad (21)$$

$$\left[P_{15}(t+\Delta t)\right]=\left[g_{03}\Delta tP_{12}(t)+g_{13}\Delta tP_{13}(t)+g_{23}\Delta tP_{14}(t)+(1-g_{30}+g_{31}+g_{32}+d_{30}+d_{31}+d_{32})\Delta tP_{15}(t)+d_{03}\Delta tP_3(t)+d_{13}\Delta tP_7(t)+d_{23}\Delta tP_{11}(t)\right]\left[P_{15}(t)\right] \quad (22)$$

Taking the limit as $\Delta t \to 0$ in Equation (7) to Equation (22), and by using the Laplace transform as well as the stated assumptions for each, Equation (7) to Equation (22) for the state probabilities, $p_i(t)$, $0 \le i \le 15$ are obtained as follows:

For Equation (7), $P_{(0)} = 1$, $P_{(1)} = P_{(2)} = P_{(3)} = P_{(4)} = P_{(8)} = P_{(12)} = 0$;

$$P_0(t) = e^{-(g_{01}+g_{02}+g_{03}+d_{01}+d_{02}+d_{03})t} \quad (23)$$

For Equation (8), $P_{(1)} = 1$, $P_{(0)} = P_{(2)} = P_{(3)} = P_{(5)} = P_{(9)} = P_{(13)} = 0$;

$$P_1(t) = e^{-(g_{10}+g_{12}+g_{13}+d_{01}+d_{02}+d_{03})t} \quad (24)$$

For Equation (9), $P_{(2)} = 1$, $P_{(0)} = P_{(1)} = P_{(3)} = P_{(6)} = P_{(10)} = P_{(14)} = 0$;

$$P_2(t) = e^{-(g_{20}+g_{21}+g_{23}+d_{01}+d_{02}+d_{03})t} \quad (25)$$

For Equation (10), $P_{(3)} = 1$, $P_{(0)} = P_{(1)} = P_{(2)} = P_{(7)} = P_{(11)} = P_{(15)} = 0$;

$$P_3(t) = e^{-(g_{30}+g_{31}+g_{32}+d_{01}+d_{02}+d_{03})t} \quad (26)$$

For Equation (11), $P_{(4)} = 1$, $P_{(0)} = P_{(5)} = P_{(6)} = P_{(7)} = P_{(8)} = P_{(12)} = 0$;

$$P_4(t) = e^{-(g_{01}+g_{02}+g_{03}+d_{10}+d_{12}+d_{13})t} \quad (27)$$

For Equation (12), $P_{(5)} = 1$, $P_{(1)} = P_{(4)} = P_{(6)} = P_{(7)} = P_{(9)} = P_{(13)} = 0$;

$$P_5(t) = e^{-(g_{10}+g_{12}+g_{13}+d_{10}+d_{12}+d_{13})t} \quad (28)$$

For Equation (13), $P_{(6)} = 1$, $P_{(2)} = P_{(4)} = P_{(5)} = P_{(7)} = P_{(10)} = P_{(14)} = 0$;

$$P_6(t) = e^{-(g_{20}+g_{21}+g_{23}+d_{10}+d_{12}+d_{13})t} \quad (29)$$

For Equation (14), $P_{(7)} = 1$, $P_{(3)} = P_{(4)} = P_{(5)} = P_{(6)} = P_{(11)} = P_{(13)} = 0$;

$$P_7(t) = e^{-(g_{30}+g_{31}+g_{32}+d_{10}+d_{12}+d_{13})t} \quad (30)$$

For Equation (15), $P_{(8)} = 1$, $P_{(0)} = P_{(4)} = P_{(9)} = P_{(10)} = P_{(11)} = P_{(12)} = 0$;

$$P_8(t) = e^{-(g_{01}+g_{02}+g_{03}+d_{20}+d_{21}+d_{23})t} \quad (31)$$

For Equation (16), $P_{(9)} = 1$, $P_{(1)} = P_{(5)} = P_{(8)} = P_{(10)} = P_{(11)} = P_{(13)} = 0$;

$$P_9(t) = e^{-(g_{10}+g_{12}+g_{13}+d_{20}+d_{23}+d_{21})t} \quad (32)$$

For Equation (17), $P_{(10)} = 1$, $P_{(2)} = P_{(6)} = P_{(8)} = P_{(9)} = P_{(11)} = P_{(14)} = 0$;

$$P_{10}(t) = e^{-(g_{20}+g_{21}+g_{23}+d_{20}+d_{21}+d_{23})t} \quad (33)$$

For Equation (18), $P_{(11)} = 1$, $P_{(3)} = P_{(7)} = P_{(8)} = P_{(9)} = P_{(10)} = P_{(15)} = 0$;

$$P_{11}(t) = e^{-(g_{30}+g_{31}+g_{32}+d_{10}+d_{21}+d_{23})t} \quad (34)$$

For Equation (19), $P_{(12)} = 1$, $P_{(0)} = P_{(4)} = P_{(8)} = P_{(13)} = P_{(14)} = P_{(15)} = 0$;

$$P_{12}(t) = e^{-(g_{01}+g_{02}+g_{03}+d_{30}+d_{31}+d_{32})t} \quad (35)$$

For Equation (20), $P_{(13)} = 1$, $P_{(1)} = P_{(5)} = P_{(9)} = P_{(12)} = P_{(14)} = P_{(15)} = 0$;

$$P_{13}(t) = e^{-(g_{10}+g_{12}+g_{13}+d_{30}+d_{31}+d_{32})t} \quad (36)$$

For Equation (21), $P_{(14)} = 1$, $P_{(2)} = P_{(6)} = P_{(10)} = P_{(12)} = P_{(13)} = P_{(15)} = 0$;

$$P_{14}(t) = e^{-(g_{20}+g_{21}+g_{23}+d_{30}+d_{31}+d_{32})t} \quad (37)$$

For Equation (22), $P_{(15)} = 1$, $P_{(3)} = P_{(7)} = P_{(11)} = P_{(12)} = P_{(13)} = P_{(14)} = 0$;

$$P_{15}(t) = e^{-(g_{30}+g_{31}+g_{32}+d_{30}+d_{31}+d_{32})t} \quad (38)$$

The availability, $A(t)$ of the WEGS at any time, $t$ is the sum of all the probabilities, thus, Equation (23) to Equation (38) which is given by Equation (39) [8] [13]:

$$A(t)=\sum_{i=1}^{n}P_i(t),\ n=16 \tag{39}$$

Substituting the probabilities into Equation (39), results in Equation (40) as follows:

$$\begin{aligned}A(t)=&\mathrm{e}^{-(g_{01}+g_{02}+g_{03}+d_{01}+d_{02}+d_{03})t}+\mathrm{e}^{-(g_{10}+g_{12}+g_{13}+d_{01}+d_{02}+d_{03})t}+\mathrm{e}^{-(g_{30}+g_{31}+g_{32}+d_{01}+d_{02}+d_{03})t}\\&+\mathrm{e}^{-(g_{01}+g_{02}+g_{03}+d_{10}+d_{12}+d_{13})t}+\mathrm{e}^{-(g_{10}+g_{12}+g_{13}+d_{10}+d_{12}+d_{13})t}+\mathrm{e}^{-(g_{20}+g_{21}+g_{23}+d_{10}+d_{12}+d_{13})t}\\&+\mathrm{e}^{-(g_{30}+g_{31}+g_{32}+d_{10}+d_{12}+d_{13})t}+\mathrm{e}^{-(g_{01}+g_{02}+g_{03}+d_{20}+d_{21}+d_{23})t}+\mathrm{e}^{-(g_{10}+g_{12}+g_{13}+d_{20}+d_{23}+d_{21})t}\\&+\mathrm{e}^{-(g_{20}+g_{21}+g_{23}+d_{20}+d_{21}+d_{23})t}+\mathrm{e}^{-(g_{30}+g_{31}+g_{32}+d_{10}+d_{21}+d_{23})t}+\mathrm{e}^{-(g_{01}+g_{02}+g_{03}+d_{30}+d_{31}+d_{32})t}\\&+\mathrm{e}^{-(g_{10}+g_{12}+g_{13}+d_{30}+d_{31}+d_{32})t}+\mathrm{e}^{-(g_{20}+g_{21}+g_{23}+d_{30}+d_{31}+d_{32})t}+\mathrm{e}^{-(g_{30}+g_{31}+g_{32}+d_{30}+d_{31}+d_{32})t}\end{aligned} \tag{40}$$

The full availability, $A_f(t)$ of the WEGS during which the electric power demand is fully met occurs at states 1, 2, 5, 6, 9, 10, 13, and 14. Therefore, the full availability, $A_f(t)$ is given by Equation (41):

$$\begin{aligned}A_f(t)&=P_1+P_2+P_5+P_6+P_9+P_{10}+P_{13}+P_{14}\\&=\mathrm{e}^{-(g_{01}+g_{02}+g_{03}+d_{01}+d_{02}+d_{03})t}+\mathrm{e}^{-(g_{10}+g_{12}+g_{13}+d_{01}+d_{02}+d_{03})t}+\mathrm{e}^{-(g_{10}+g_{12}+g_{13}+d_{10}+d_{12}+d_{13})t}\\&\quad+\mathrm{e}^{-(g_{20}+g_{21}+g_{23}+d_{10}+d_{12}+d_{13})t}+\mathrm{e}^{-(g_{10}+g_{12}+g_{13}+d_{20}+d_{23}+d_{21})t}+\mathrm{e}^{-(g_{20}+g_{21}+g_{23}+d_{20}+d_{21}+d_{23})t}\\&\quad+\mathrm{e}^{-(g_{10}+g_{12}+g_{13}+d_{30}+d_{31}+d_{32})t}+\mathrm{e}^{-(g_{20}+g_{21}+g_{23}+d_{30}+d_{31}+d_{32})t}\end{aligned} \tag{41}$$

The partial availability, $A_p(t)$ of the WEGS during which the electric power demand is not fully met occurs at states 0, 3, 4, 7, 8, 11, 12, and 15. Therefore, the partial availability, $A_p(t)$ is given by Equation (42):

$$\begin{aligned}A_p(t)&=P_0+P_3+P_4+P_7+P_8+P_{11}+P_{12}+P_{15}\\&=\mathrm{e}^{-(g_{01}+g_{02}+g_{03}+d_{01}+d_{02}+d_{03})t}+\mathrm{e}^{-(g_{30}+g_{31}+g_{32}+d_{01}+d_{02}+d_{03})t}+\mathrm{e}^{-(g_{01}+g_{02}+g_{03}+d_{10}+d_{12}+d_{13})t}\\&\quad+\mathrm{e}^{-(g_{30}+g_{31}+g_{32}+d_{10}+d_{12}+d_{13})t}+\mathrm{e}^{-(g_{01}+g_{02}+g_{03}+d_{20}+d_{21}+d_{23})t}+\mathrm{e}^{-(g_{30}+g_{31}+g_{32}+d_{10}+d_{21}+d_{23})t}\\&\quad+\mathrm{e}^{-(g_{01}+g_{02}+g_{03}+d_{30}+d_{31}+d_{32})t}+\mathrm{e}^{-(g_{30}+g_{31}+g_{32}+d_{30}+d_{31}+d_{32})t}\end{aligned} \tag{42}$$

The assumed transition rates were used to compute the possible probabilities at the various transition states during an interval of one hour up to the fourth hour which is given by Table 4 using Equation (23) to Equation (39). A transition state probability graph based on Table 4 for the WEGS is given by Figure 9.

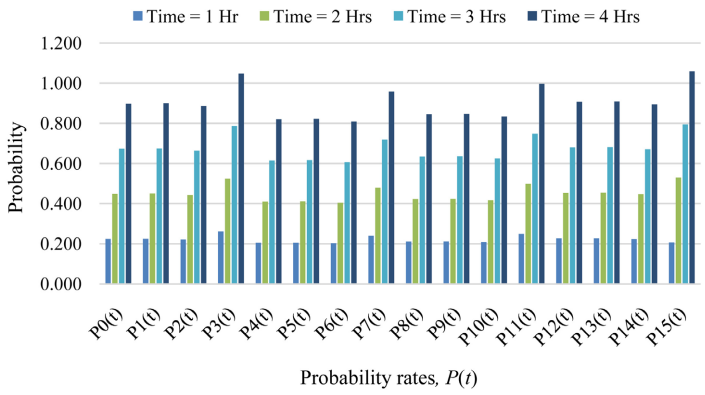


Figure 9. A transition state probability graph for the combined WEGS and the power demand.

**Table 4.** Probabiliites of the combined WEGS and the power demands at the various states and at different times.

| States | Probabilities, $P(t)$ | Time, $T_1 = 1$ | Time, $T_2 = 2$ | Time, $T_3 = 3$ | Time, $T_4 = 4$ |
|---|---|---|---|---|---|
| 0 | $p_0(t)$ | 0.224 | 0.449 | 0.673 | 0.898 |
| 1 | $p_1(t)$ | 0.225 | 0.450 | 0.675 | 0.900 |
| 2 | $p_2(t)$ | 0.221 | 0.443 | 0.664 | 0.885 |
| 3 | $p_3(t)$ | 0.262 | 0.524 | 0.786 | 1.049 |
| 4 | $p_4(t)$ | 0.205 | 0.410 | 0.615 | 0.821 |
| 5 | $p_5(t)$ | 0.206 | 0.411 | 0.617 | 0.822 |
| 6 | $p_6(t)$ | 0.202 | 0.405 | 0.607 | 0.809 |
| 7 | $p_7(t)$ | 0.240 | 0.479 | 0.719 | 0.958 |
| 8 | $p_8(t)$ | 0.211 | 0.423 | 0.634 | 0.846 |
| 9 | $p_9(t)$ | 0.212 | 0.424 | 0.635 | 0.847 |
| 10 | $p_{10}(t)$ | 0.208 | 0.417 | 0.625 | 0.834 |
| 11 | $p_{11}(t)$ | 0.249 | 0.499 | 0.748 | 0.997 |
| 12 | $p_{12}(t)$ | 0.227 | 0.453 | 0.680 | 0.907 |
| 13 | $p_{13}(t)$ | 0.227 | 0.454 | 0.682 | 0.909 |
| 14 | $p_{14}(t)$ | 0.224 | 0.447 | 0.671 | 0.894 |
| 15 | $p_{15}(t)$ | 0.265 | 0.530 | 0.794 | 1.059 |

The mean or average instantaneous electric power generation, $G_t$ by the WEGS at time, $t$ based on **Table 3** is given as follows [14] [15]:

$$\begin{aligned} G_t &= \sum_{i=0}^{15} g_i p_i(t) \\ &= 10p_0(t) + 10p_1(t) + 10p_2(t) + 10p_3(t) + 120p_4(t) + 120p_5(t) \\ &\quad + 120p_6(t) + 120p_7(t) + 200p_8(t) + 200p_9(t) + 200p_{10}(t) \\ &\quad + 200p_{11}(t) + 40p_{12}(t) + 40p_{13}(t) + 40p_{14}(t) + 70p_{15}(t) \end{aligned} \tag{43}$$

Assuming the average electric power demand is 90 MW (which is the average of the four electric power demands at the various transition states), the WEGS mean instantaneous generation deficiency, $G_{def}$ is obtained as follows [14] [15]:

$$G_{def} = \sum_{i=0}^{3} p_i(t) \max(d_{av} - g_i, 0) = 80p_0(t) + 30p_1(t) + 50p_3(t) \tag{44}$$

where, $G_{def}$ is the generation deficiency, $d_{av}$ is average electric power demand,

$p_i(t)$ is the probability at a particular state, $g_i(t)$ is the electric power generation at a particular state. A graph of mean instantaneous generation $G_t$ and mean instantaneous generation deficiency, $G_{def}$ is given by **Figure 10**. The expected energy not supplied (EENS) or loss of energy expectation (LOEE) also known expected unserved energy (EUE) is a measure of the amount of electricity demand (in MWh in a given year) expected to be lost when demand exceeds the available generation. Therefore, the expected energy not supplied (EENS) or expected unserved energy (EUE) to the consumers during the 24-hour operation of the WEGS is as follows [14] [15]:

$$\text{EENS} = \int_0^{24} D_{def}\,\mathrm{d}t = \int_0^{24} 80\mathrm{d}t + 30\mathrm{d}t + 50\mathrm{d}t = 3840000 \text{ kWh} \tag{45}$$

The annual expected energy not supplied (EENS) is computed as follows [14] [15]:

$$\text{EENS} = \int_0^{8760} D_{def}\,\mathrm{d}t = \int_0^{8760} 80\mathrm{d}t + 30\mathrm{d}t + 50\mathrm{d}t = 1401600 \text{ kWh} \tag{46}$$

The surplus electric power generation, $G_{surplus}$ by the WEGS at time, $t$ is given by [15]:

$$G_{surplus} = \sum_{i=0}^{3} p_i(t)\max(g_i - d_{av}, 0) = 110\,p_2(t) \tag{47}$$

$$G_{surplus} = \int_0^{24} 110\mathrm{d}t = 2640000 \text{ kWh} \tag{48}$$

Based on **Table 1** and **Table 2** for the assumed power generation and load demand at the various transition states, the expected demand not supplied (EDNS) which is the difference between the expected power to be generated and the expected power demand by the consumers, is obtained at each transition state as given in **Table 5** [16]. Graphs based on the various transition states are depicted by **Figures 11-14** respectively.

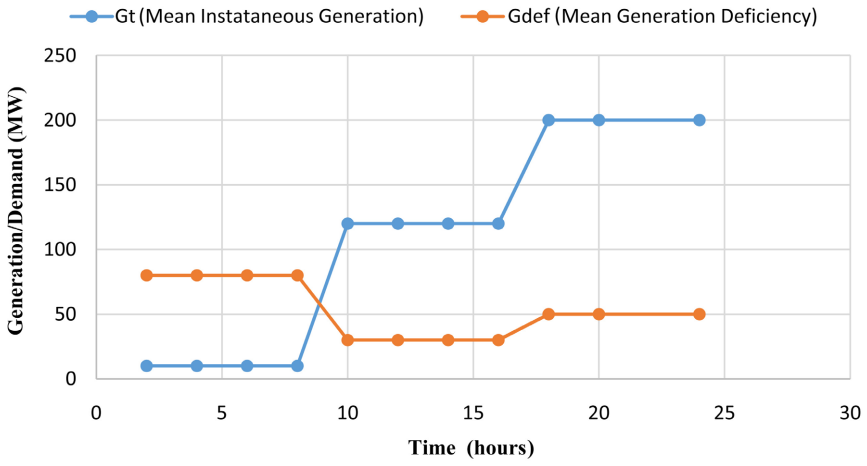


**Figure 10.** A graph of mean instantaneous generation and mean instantaneous generation deficiency.

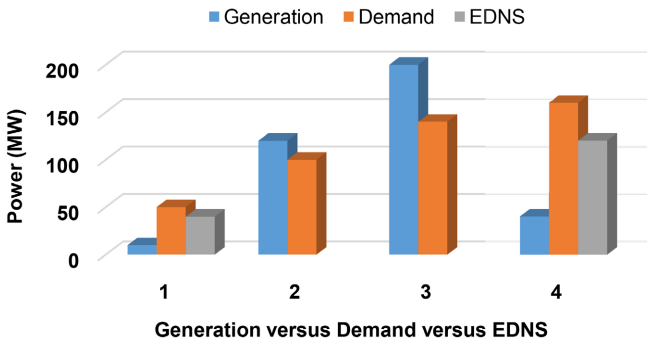


Figure 11. Generation versus demand versus EDNS at state 0.

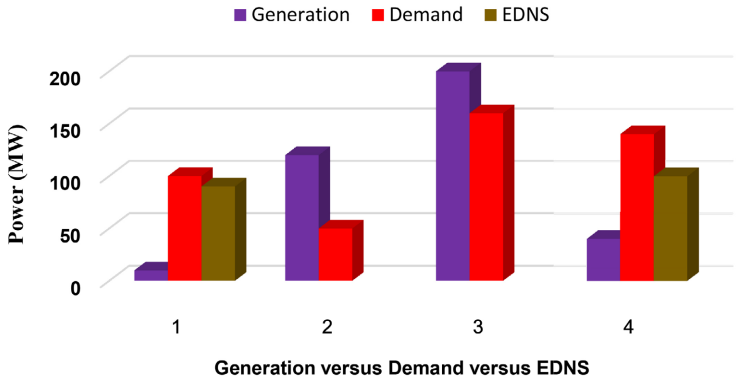


Figure 12. Generation versus demand versus EDNS at state 1.

Table 5. Power generation, power demand and EDNS.

| States | Generation | Demand | EDNS |
|---|---|---|---|
| 0 | 10 | 50 | 40 |
| | 120 | 100 | x |
| | 200 | 140 | x |
| | 40 | 160 | 120 |
| 1 | 10 | 100 | 90 |
| | 120 | 50 | x |
| | 200 | 160 | x |
| | 40 | 140 | 100 |
| 2 | 10 | 140 | 130 |
| | 120 | 160 | 40 |
| | 200 | 50 | x |
| | 40 | 100 | 60 |
| 3 | 10 | 160 | 150 |
| | 120 | 140 | 20 |
| | 200 | 100 | x |
| | 40 | 50 | 10 |

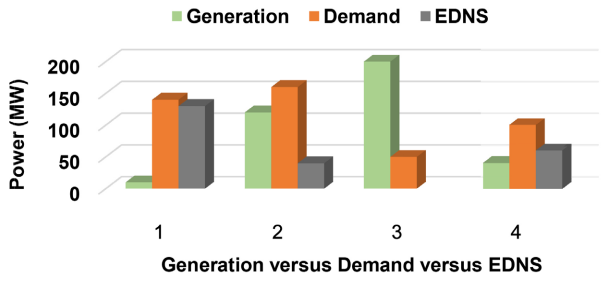


**Figure 13.** Generation versus demand versus EDNS at state 2.

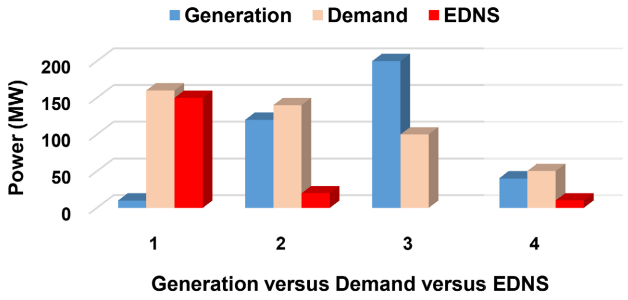


**Figure 14.** Generation versus demand versus EDSN at state 3.

## 4. Conclusion

Reliability analysis of WEGS and a proposed varying load was carried out using various electric power generation related indices to ascertain how a large-scale wind farm comprising WTs will behave under varying wind speeds and varying load conditions. It was obvious from the analysis that during certain transition states, the electric power demand will be more than that of the electric power generation. And during certain transition states, the electric power generation will exceed that of the power demand. It was also clear from the analysis that the probability that the WEGS system will be in a particular state is fairly high indicating that the electric power demand during that particular state is likely to be met. On the other hand, some transition states probabilities which is an indication that the electric power load during those transition states might not be met. The mean instantaneous generation graph and mean generation deficiency graph have shown that during the early hours of WEGS operation, there will be some generation deficiencies. However, as time progresses, the mean instantaneous power generation will exceed the mean electric power demand. The uniqueness of the study is that it brought to bear the behavior of a large-scale WEGS under different wind speeds, and a varying load conditions it is supplying. Due to the volatility of the price of fossil fuel and instability around the globe, this study is intended to examine how a future WEGS and other renewable energy resources for power generation can be operated on a large scale in the same manner like that of the conventional power generation system without excessive instability situations. A further study is proposed to ascertain how the model will behave when the model assumptions are varied and the transition rates as well.

## Conflicts of Interest

The authors declare no conflicts of interest regarding the publication of this paper.

## References


[1] Kim, D. and Hur, J. (2017) Stochastic Prediction of Wind Generating Resources Using the Enhanced Ensemble Model for Jeju Island's Wind Farms in South Korea. *Sustainability*, **9**, Article 817. https://doi.org/10.3390/su9050817

[2] Su, H. and Chen, L. (2021) Stochastic Model Analysis of Preventive Maintenance based on Wind Turbine Gearbox Space-Time Evolution. *Journal of Applied Science and Engineering*, **255**, 721-732.

[3] Zhu, C. and Li, Y. (2018) Stability Control and Reliable Performance of Wind Turbines. IntecOpen, London, 169-175.

[4] Ding, Y., Singh, C., Goel, L., Ostergaard, J. and Wang, P. (2014) Short-Term and Medium-Term Reliability Evaluation for Power Systems with High Penetration of Wind Power. *IEEE Transactions on Sustainable Energy*, **5**, 896-906. https://doi.org/10.1109/TSTE.2014.2313017

[5] Yusuf, I., Ismail, A L. and Ali, U.A. (2020) Reliability Analysis of Communication Network System with Redundant Relay Station under Partial and Complete Failure. *Journal of Mathematics and Computer Science*, **10**, 863-880.

[6] Ozturk, S., Fthenakis, V.M. and Faulstich, S. (2018) Failure Modes, Effects and Criticality Analysis for Wind Turbines Considering Climatic Regions and Comparing Geared and Direct Drive Wind Turbines. *Energie*s, **11**, Article 2317. https://doi.org/10.3390/en11092317

[7] Hou, K., Jia, H., Xu, X., Liu, Z. and Jiang, Y. (2016) A Continuous Time Markov Chain Based Sequential Analytical Approach for Composite Power System Reliability Assessment. *IEEE Transactions on Power Systems*, **31**, 738-748, https://doi.org/10.1109/TPWRS.2015.2392103

[8] Zuo, W. and Li, K. (2021) Three-state Markov Chain Based Reliability Analysis of Complex Traction Power Supply Systems. 5*th IEEE International Conference on System Reliability and Safety*, Palermo, 24-26 November 2021, 74-79. https://doi.org/10.1109/ICSRS53853.2021.9660623

[9] Xiao, Z., Zhao, Q., Yang, X. and Zhu, A. (2020) A Power Performance Online Assessment Method of a Wind Turbine Based on the Probabilistic Area Metric. *Applied Sciences*, **10**, Article 3268. https://doi.org/10.3390/app10093268

[10] Roy, A. and Chatterjee, K. (2018) Reliability Analysis of a Multi-State Wind Farm Using Markov Process. *Safety and Reliability*, **37**, 3-24. https://doi.org/10.1080/09617353.2017.1418811

[11] Singh, C., Jirutitijaroen, P. and Mitra, J. (2019) Electric Power Grid Reliability Evaluation—Models and Methods. John Wiley and Sons, Inc., Hoboken, New Jersey, USA, 117-160. https://doi.org/10.1002/9781119536772

[12] Ibe, O. (2013) Markov Processes for Stochastic Modelling. 2nd Edition, Elsevier, London. https://doi.org/10.1016/B978-0-12-407795-9.00015-3

[13] Kalaiarasi, S., Anita, A.M. and Geethanjalii, R. (2017) Analysis of System Reliability Using Markov Technique. *Global Journal of Pure and Applied Mathematics*, **13**, 5265-5273.

[14] Levitina, G., Xing, L. and Huang, H.Z. (2019) Dynamic Availability and Perform-

ance Deficiency of Common Bus Systems with Imperfectly Repairable Components. *Reliability Engineering and System Safety*, **189**, 58-66. https://doi.org/10.1016/j.ress.2019.04.007

[15] Lisnianskia, A., Frenkel, I. and Khvatskin, L. (2017) On Sensitivity Analysis of Aging Multi-State System by Using LZ-Transform. *Reliability Engineering and System Safety*, **166**, 99-108. https://doi.org/10.1016/j.ress.2016.12.001

[16] Al-Shaalan, A.M. (2019) Reliability Evaluation of Power Systems. IntecOpen, London, United Kingdom. https://doi.org/10.5772/intechopen.85571